31st Congress of the International Council of the Aeronautical Sciences

Belo Horizonte, Brazil; September 09-14, 2018

CLOSED-LOOP SYSTEM IDENTIFICATION OF A LARGE FLEXIBLE AIRCRAFT USING SUBSPACE METHODS

Raphaela Carvalho Machado Gonçalves Barbosa* , **Luiz Carlos Sandoval Góes****
*Instituto Tecnológico de Aeronáutica -ITA , **Instituto Tecnológico de Aeronáutica -ITA

Keywords: *system identification, closed-loop, subspace method, flexible aircraft*

Abstract

This work presents a methodology for system identification of a large flexible aircraft operating in closed-loop. The feedback in some cases is necessary because the system in open-loop is unstable or because a controller, known or not, is present on system and is not possible to removed it. The synthetic data of a nonlinear dynamic to the aircraft considering three symmetric and two anti-symmetric flexible modes are used in the identification algorithm. The identification algorithm is a non iterative subspace method well applied for both open and closed-loop data. The preliminary results suggest a representative model for the aircraft, obtaining the state-space matrices that are of very interest and used for control system analysis and design.

1 Introduction

The identification of aircrafts with flexible structure have been investigated [1], [2] mainly due to the coupling of dynamics. In [3] a study about the influence of aircraft loads is presented in order to include known flexible effects because of the new structural designs concepts.

In this way, dynamic models of aircrafts contained the efforts of aerodynamics are needed to system analysis as well as to closed-loop control system design based on an accuracy aircraft model [4]. Techniques to estimate the aerodynamics coefficients have been applied and may be obtained, for example, from wind-tunnel tests while others may be estimated via numerical techniques. In both cases, efforts are needed to determine aerodynamics coefficients with confidence [5], [6].

Others approaches that have been applied to obtained representative models are the subspace methods [7]. Although they are referred to as black-box models, they offers an advantageous that are not an optimization algorithm and do not suffer from the inconveniences encountered in applying this methods, being an efficient alternative for system identification.

In cases of closed-loop operation, some classical methods, e.g., the prediction error method (PEM) and the output error method (OEM), may be fail and produce biased estimates. So, another class of identification algorithms based on subspace theory have been applied, just to deals with some difficulties that the feedback provides [8].

In this way this work presents an identification procedure to identify a flexible aircraft in closed-loop operation. The follows sections describe the problem formulation and the results obtained from closed-loop simulated data.

2 Problem formulation

The subsection 2.1 presents the equations of motion of a large flexible aircraft well known in the literature as Rockwell-B1 aircraft [9]. Some mechanical characteristics used for simulation and the flexible modes are presented. The subsection 2.2 describes a flight condition used to obtain a linear model, in which the eigenvalues are used to distinguish the modes of longitudinal and lateral-directional dynamics, including the flex-

ible modes. An identification procedure is described in subsection 2.3.

2.1 The aircraft dynamic

The mathematical model used to develop the simulation is available in the open literature [10] and a source-code implemented by the author is in MATLAB/SIMULINK. The MIMO system, shown in Fig.1, has seven control-surfaces deflections and the propulsion thrust acts along the vehicle's fuselage, in X-axis. The propulsion thrust is not able to generate moment.

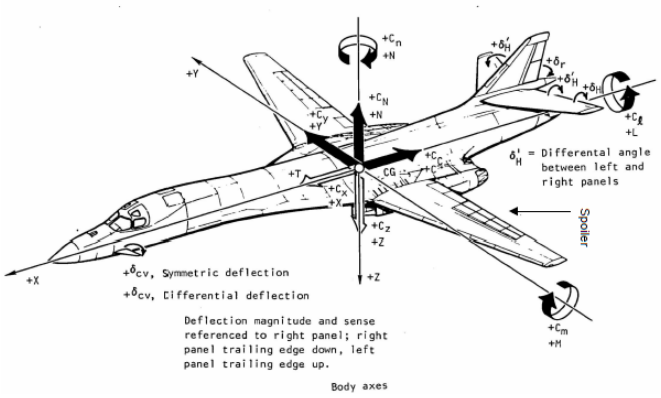

Fig. 1 Rockwell-B1 aircraft.

The mechanical characteristics, mass and inertial properties of the aircraft are summarized in Tab.1, while the modal frequencies and the generalized masses are given in Tab.2.

Table 1 Mechanical characteristics.

Wing geometry	Mass and Inertias
S=1,946 ft^2	m=288,017 lb
$\bar{c}$=15.3 ft	I_{xx}=950 $\times$ 10^3 slug.ft^2
b=70 ft	I_{yy}=6,400 $\times$ 10^3 slug.ft^2
Λ=65 deg	I_{zz}=7,100 $\times$ 10^3 slug.ft^2
-	I_{xz}=-52.7 $\times$ 10^3 slug.ft^2
-	I_{xy}=I_{yz}=0

The aerodynamics efforts acting in longitudinal and lateral-directional dynamics are governing by forces and moments equations.

Considering this aircraft, the aerodynamic forces coefficients are,

Table 2 Vibrations modal frequencies and generalizes masses.

Symmetric modes		Anti-symmetric modes	
ω (rad/s)	μ (sl-ft^2)	ω (rad/s)	μ (sl-ft^2)
12.6	184	12.9	28,991
14.1	9,587	16.5	136
21.2	1,334	-	-

$$C_X = C_{X0} + C_{X_{\delta H}}\delta_H + C_{X_q}\frac{q\bar{c}}{2V} + C_{X_{\delta sp}}|\delta_{sp}| \quad (1)$$

$$\begin{aligned} C_Y = {} & C_{Y_\beta}\beta + C_{Y_{\delta RU}}\delta_{RU} + C_{Y_{\delta RL}}\delta_{RL} + C_{Y_{\delta H}}\delta_H + \ldots \\ & C_{Y_{\delta sp}}|\delta_{sp}| + C_{Y_{cvanti}} + \ldots \\ & C_{Y_{\eta_4}}\eta_4 + \frac{C_{Y_{\dot{\eta}_4}}}{u}\dot{\eta}_4 + C_{Y_{\eta_5}}\eta_5 + \frac{C_{Y_{\dot{\eta}_5}}}{u}\dot{\eta}_5 \end{aligned} \quad (2)$$

$$\begin{aligned} C_Z = {} & C_{Z_0} + C_{Z_{\delta H}}\delta_H + C_{Z_q}\frac{q\bar{c}}{2V} + C_{Z_{\delta sp}}|\delta_{sp}| + \ldots \\ & C_{Z_{\delta_{cvsym}}}(\delta_{cvsym} + 0.866 - \varepsilon) + \ldots \\ & C_{Z_{\eta_1}}\eta_1 + \frac{C_{Z_{\dot{\eta}_1}}}{u}\dot{\eta}_1 + C_{Z_{\eta_2}}\eta_2 + \frac{C_{Z_{\dot{\eta}_2}}}{u}\dot{\eta}_2 \\ & + C_{Z_{\eta_3}}\eta_3 + \frac{C_{Z_{\dot{\eta}_3}}}{u}\dot{\eta}_3 \end{aligned} \quad (3)$$

and the aerodynamic moments coefficients are,

$$\begin{aligned} C_l = {} & C_{l_\beta}\beta + C_{l_{\delta RU}}\delta_{RU} + C_{l_{\delta RL}}\delta_{RL} + C_{l_{\delta DH}}\delta_{DH} + \ldots \\ & C_{l_{\delta sp}}\delta_{sp} + C_{l_p}\frac{pb}{2V} + C_{l_r}\frac{rb}{2V} + \ldots \\ & C_{l_{\eta_4}}\eta_4 + \frac{C_{l_{\dot{\eta}_4}}}{u}\dot{\eta}_4 + C_{l_{\eta_5}}\eta_5 + \frac{C_{l_{\dot{\eta}_5}}}{u}\dot{\eta}_5 \end{aligned} \quad (4)$$

$$\begin{aligned} C_m = {} & C_{m_0} + C_{m_{\delta H}}\delta_H + C_{m_{\dot{\alpha}}}\frac{\dot{\alpha}\bar{c}}{2V} + C_{m_q}\frac{q\bar{c}}{2V} + \ldots \\ & C_{m_{\delta sp}}|\delta_{sp}| + C_{m_{\delta_{cvsym}}}(\delta_{cvsym} + 0.806 - \varepsilon) + \ldots \\ & C_{m_{\eta_1}}\eta_1 + \frac{C_{m_{\dot{\eta}_1}}}{u}\dot{\eta}_1 + C_{m_{\eta_2}}\eta_2 + \frac{C_{m_{\dot{\eta}_2}}}{u}\dot{\eta}_2 + \ldots \\ & C_{m_{\eta_3}}\eta_3 + \frac{C_{m_{\dot{\eta}_3}}}{u}\dot{\eta}_3 \end{aligned} \quad (5)$$

$$\begin{aligned} C_n = {} & C_{n_\beta}\beta + C_{n_{\delta RU}}\delta_{RU} + C_{n_{\delta RL}}\delta_{RL} + C_{n_{\delta H}}\delta_H + \ldots \\ & C_{n_{\delta sp}}\delta_{sp} + \frac{69.7}{136.7}C_{Y_{cvanti}} + C_{l_{\eta_4}}\eta_4 + \frac{C_{l_{\dot{\eta}_4}}}{u}\dot{\eta}_4 + \ldots \\ & C_{l_{\eta_5}}\eta_5 + \frac{C_{l_{\dot{\eta}_5}}}{u}\dot{\eta}_5 \end{aligned} \quad (6)$$

The generalized forces coefficients due to three symmetric flexible modes can be expressed

as

$$
\begin{aligned}
C_{Q_1} &= C_{Q_{1\alpha}}\alpha + \frac{1}{u}C_{Q_{1q}}q + C_{Q_{1\delta_{sp}}}|\delta_{sp}| + C_{Q_{1\delta_H}}\delta_H + \ldots \\
&\quad C_{Z_{\delta_{cvsym}}}\frac{0.56}{15.3}(\delta_{cvsym} + 0.866 \times 57.3 - \varepsilon) + \ldots \\
&\quad C_{Q_{1\eta_1}}\eta_1 + \frac{1}{u}C_{Q_{1\dot{\eta}_1}}\dot{\eta}_1 + C_{Q_{1\eta_2}}\eta_2 + \frac{1}{u}C_{Q_{1\dot{\eta}_2}}\dot{\eta}_2 + \ldots \\
&\quad C_{Q_{1\eta_3}}\eta_3 + \frac{1}{u}C_{Q_{1\dot{\eta}_3}}\dot{\eta}_3 \qquad (7) \\
C_{Q_2} &= C_{Q_{2\alpha}}\alpha + \frac{1}{u}C_{Q_{2q}}q + C_{Q_{2\delta_{sp}}}|\delta_{sp}| + \ldots \\
&\quad C_{Q_{2\delta_H}}\delta_H + C_{Z_{\delta_{cvsym}}}\frac{0.56}{15.3}(\delta_{cvsym} + \frac{0.866}{57.3} - \varepsilon) + \ldots \\
&\quad C_{Q_{2\eta_1}}\eta_1 + \frac{1}{u}C_{Q_{2\dot{\eta}_1}}\dot{\eta}_1 + C_{Q_{2\eta_2}}\eta_2 + \frac{1}{u}C_{Q_{2\dot{\eta}_2}}\dot{\eta}_2 + \ldots \\
&\quad C_{Q_{2\eta_3}}\eta_3 + \frac{1}{u}C_{Q_{2\dot{\eta}_3}}\dot{\eta}_3 \qquad (8) \\
C_{Q_3} &= C_{Q_{3\alpha}}\alpha + \frac{1}{u}C_{Q_{3q}}q + C_{Q_{3\delta_{sp}}}|\delta_{sp}| + \ldots \\
&\quad C_{Q_{3\delta_H}}\delta_H + C_{Z_{\delta_{cvsym}}}\frac{0.4}{15.3}(\delta_{cvsym} + \frac{0.866}{57.3} - \varepsilon) + \ldots \\
&\quad C_{Q_{3\eta_1}}\eta_1 + \frac{C_{Q_{3\dot{\eta}_1}}}{u}\dot{\eta}_1 + C_{Q_{3\eta_2}}\eta_2 + \frac{1}{u}C_{Q_{3\dot{\eta}_2}}\dot{\eta}_2 + \ldots \\
&\quad C_{Q_{3\eta_3}}\eta_3 + \frac{1}{u}C_{Q_{3\dot{\eta}_3}}\dot{\eta}_3 \qquad (9)
\end{aligned}
$$

and the generalized forces coefficients due to two anti-symmetric modes can be expresses as

$$
\begin{aligned}
C_{Q_4} &= C_{Q_{4\beta}}\beta + C_{Q_{4RU}}\delta_{RU} + + C_{Q_{4RL}}\delta_{RL} + \ldots \\
&\quad C_{Q_{4DH}}\delta_{DH} + \frac{1}{u}C_{Q_{4p}}p + \frac{1}{u}C_{Q_{4r}}r + \ldots \\
&\quad \frac{0.7}{15.3}C_{Q_{4(\alpha,\delta_{cvanti})}} + C_{Q_{4\eta_4}}\eta_4 + \frac{1}{u}C_{Q_{4\dot{\eta}_4}}\dot{\eta}_4 + \ldots \\
&\quad C_{Q_{4\eta_5}}\eta_5 + \frac{1}{u}C_{Q_{4\dot{\eta}_5}}\dot{\eta}_5 \qquad (10) \\
C_{Q_5} &= C_{Q_{5\beta}}\beta + C_{Q_{5RU}}\delta_{RU} + + C_{Q_{5RL}}\delta_{RL} + \ldots \\
&\quad C_{Q_{5DH}}\delta_{DH} + C_{Q_{5sp}}\delta_{sp} + \frac{1}{u}C_{Q_{5p}}p + \ldots \\
&\quad \frac{1}{u}C_{Q_{5r}}r + \frac{0.55}{15.3}C_{Q_{4(\alpha,\delta_{cvanti})}} + \\
&\quad C_{Q_{5\eta_4}}\eta_4 + \frac{1}{u}C_{Q_{5\dot{\eta}_4}}\dot{\eta}_4 + \\
&\quad C_{Q_{5\eta_5}}\eta_5 + \frac{1}{u}C_{Q_{5\dot{\eta}_5}}\dot{\eta}_5 \qquad (11)
\end{aligned}
$$

where the definitions of the total force are obvious, according to the literature [11].

2.2 A flight condition

The nonlinear model was linearized about the flight condition of straight and level cruise at an altitude of 5000 ft, or 1524 m, and at an velocity of 0.6 Mach, or 658,27 m/s. The Tab. 3 summarizes the flight condition.

Table 3 Equilibrium condition for a straight and level cruise.

p (deg/s)	0	F (kN)	164.78
q (deg/s)	0	δ_H (deg)	-6.62
r (deg/s)	0	δ_{sp}	0
V (m/s)	658.26	δ_H	0
α (deg)	0.73	δ_{DH}	0
β (deg)	0	δ_{RU}	0
ϕ (deg)	0	δ_{RL}	0
θ (deg)	0.73	δ_{cvsym}	0
H (m)	1,524	δ_{cvanti}	0
η_1 (deg)	34.61	$\dot{\eta}_1$ (deg/s)	0
η_2 (deg)	2.48	$\dot{\eta}_2$ (deg/s)	0
η_3 (deg)	-3.16	$\dot{\eta}_3$ (deg/s)	0
η_4 (deg)	0	$\dot{\eta}_4$ (deg/s)	0
η_5 (deg)	0	$\dot{\eta}_5$ (deg/s)	0

The eigenvalues of dynamic matrix obtained from linearizion procedure is plotted in Fig.2. It's possible to note that not exist a significant interaction between the rigid and flexible dynamics. So, the problems due to coupling the dynamics seems to be avoided but not least the problem formulation of to recover the flexible system dynamic remains.

2.3 The identification procedure

The identification of multivariable systems in closed-loop operation has been investigated in the last decades since open-loop system are unstable or when a controller already is mounted in the system and it's not possible remove it. So, an identification procedure in closed-loop have to be applied in order to recover the system dynamic and at the same time avoid the biasing of estimates, due to correlation between the input and the noise caused by feedback action.

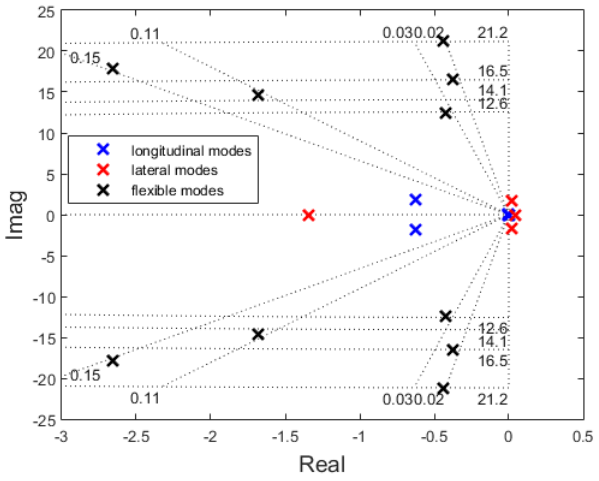

Fig. 2 Eigenvalues of the linearized dynamics.

Table 4 Parameters of the eigenvalues of the linearized dynamics: natural frequency w_n and damping factor ξ.

eigenvalues	w_n	ξ	mode
$-0.64 \pm j1.78$	1.9	0.34	short period
$-0.0065 \pm j0.07$	0.07	0.09	phugoid
0	-	-	due altitude
eigenvalues	w_n	ξ	mode
0.0286	0	-1	spiral
-1.33	0	1	roll
$-0.0021 \pm j1.68$	1.68	0.001	dutch roll
eigenvalues	w_n	ξ	mode
$-0.42 \pm j12.39$	12.4	0.03	1 sym.
$-2.65 \pm j17.84$	18	0.14	2 sym.
$-0.43 \pm j21.24$	21.2	0.02	3 sym.
$-1.68 \pm j14.67$	14.8	0.11	4 anti.
$-0.37 \pm j16.59$	16.6	0.02	5 anti.

There are three approaches described in [7] just for system identification applied to closed-loop data with a typical configuration as shown in Fig.3. The first approach ignores the existence of the feedback and applying the open-loop identification methods directly in input-output data (u,y). Since the correlation between the input signal and the noise is relatively small, the results obtained are satisfactory.

The second approach considers that the controller is known and it's possible to calculate the system dynamic from transfer function of (r,y) data. And the third approach uses data of input, output and reference signal just to identify the plant and the controller when both are unknown. It's should also be noted that choice what approach can be applied depends on the purpose of the model.

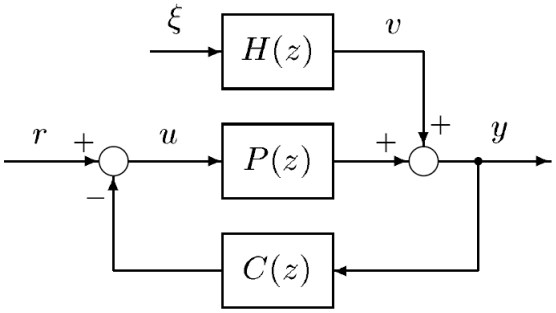

Fig. 3 A feedback system.

In this work, the first approach is applied in the identification procedure, since a controller dynamics is not the most important role compared with the many parameters involved in the equations of motion which includes the aerodynamic coefficients.

The subspace method presented in [12] was implemented in MATLAB script and is applied in this work for system identification of the flexible aircraft. The identification procedure concerns in applying of the DSR algorithm [13] to input-output data (u,y) and identify a linear innovation model,

$$\begin{aligned} \mathbf{x}_{k+1} &= \mathbf{A}\mathbf{x}_k + \mathbf{B}\mathbf{u}_k + \mathbf{K}\varepsilon_k \\ \mathbf{y}_k &= \mathbf{C}\mathbf{x}_k + \varepsilon_k \end{aligned} \tag{12}$$

where $\mathbf{x}_k$ is the system states vector, $\mathbf{u}_k$ is the input vector, $\mathbf{y}_k$ is the output vector and ε_k is the innovation method. The identification problem consists in determine the model matrices $\mathbf{A}$, $\mathbf{B}$ and $\mathbf{C}$ and the Kalman gain $\mathbf{K}$.

3 Results

The closed-loop system was performed with a pitch-rate control augmentation systems design,

namely pitch-rate CAS, in order to became more fast the closed-loop dynamics, providing a large damping, and generating synthetic data for identification based on a typical configuration of feedback control. The SIMULINK diagrams for the pitch-axis CAS is shown in Fig.4. The pitch-rate CAS is an integrative controller, performing feeding back both the pitch-rate and attack angle.

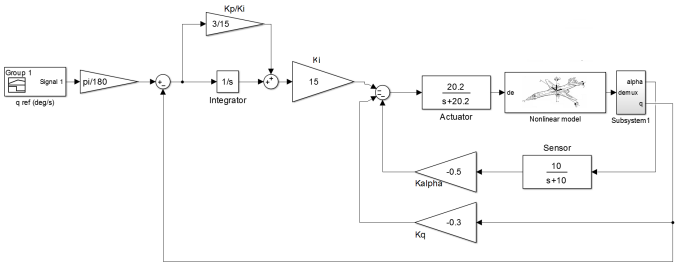

Fig. 4 Pitch-rate CAS design implemented in MATLAB/SIMULINK.

A typical doublet signal was applied to the system just to evaluated the closed-loop operation. In open-loop the phugoidal mode has a settling time about 400 seconds while in closed loop about 6 seconds.

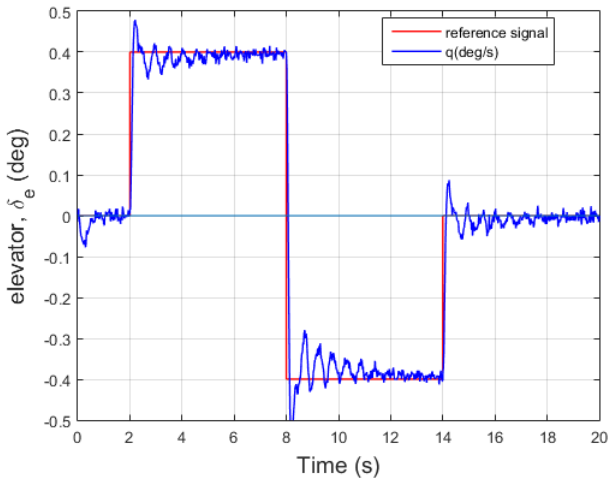

Fig. 5 Closed-loop operation: a pitch-rate CAS control.

The following sections present the results of the closed-loop identification.

3.1 Subspace algorithm: DSR (combined deterministic and stochastic system identification and realization)

The DSR algorithm proposed by [12] is a subspace method composed basically by two steps. In the first step, the experimental data is divided in two parts, a deterministic part $\mathbf{y}^d_{J/1}$ and an innovation part $\varepsilon_{J/1}$. In the second step, a discrete state-space model is obtained solving a deterministic identification problem according to [14].

An alternative procedure to solve a deterministic problem was performed applying the N4SID (numerical algorithms for subspace state space system identification) algorithm [13]. Results indicate that the methodology is a viable alternative to solve the deterministic identification problem. The block diagram referred to the algorithm DSR is shown in Fig.6.

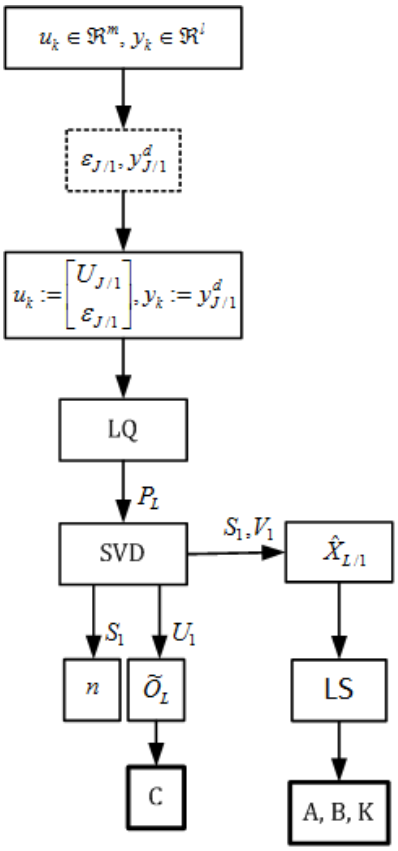

Fig. 6 DSR algorithm using the N4SID to solve the deterministic identification problem.

The deterministic component is obtained by

$$\mathbf{y}^d_{J/1} = \mathbf{Y}_{J/1} / \begin{bmatrix}\mathbf{U}_{0/J}\\ \mathbf{Y}_{0/J}\end{bmatrix} \quad (13)$$

and the innovation sequence is estimate by

$$\varepsilon_{J/1} = \mathbf{Y}_{J/1} - \mathbf{Y}_{J/1} / \begin{bmatrix}\mathbf{U}_{0/J}\\ \mathbf{Y}_{0/J}\end{bmatrix} \quad (14)$$

The Hankel matrices from input-output data used to uncorrelate the noise and the future input signal, are define as

$$U_{0/J+1} = \begin{bmatrix}\mathbf{U}_{0/J}\\ \mathbf{U}_{J/1}\end{bmatrix} \quad (15)$$
$$Y_{0/J+1} = \begin{bmatrix}\mathbf{Y}_{0/J}\\ \mathbf{Y}_{J/1}\end{bmatrix}$$

After the uncorrelation process, a determination of the system matrices may be obtained solving the following determinism identification problem,

$$\mathbf{x}_{k+1} = \mathbf{A}\mathbf{x}_k + \begin{bmatrix}\mathbf{B} & \mathbf{K}\end{bmatrix}\begin{bmatrix}\mathbf{u}_k\\ \varepsilon_k\end{bmatrix} \quad (16)$$
$$\mathbf{y}^d_k = \mathbf{C}\mathbf{x}_k$$

with a new data set being defined as

$$\mathbf{u}_k := \begin{bmatrix}\mathbf{U}_{J/1}\\ \varepsilon_{J/1}\end{bmatrix} \quad (17)$$
$$\mathbf{y}_k := \mathbf{y}^d_{J/1}$$

where $k = J, J+1, J+2, ..., N-1$ and the number of samples is $N := N - J$.

The closed-loop system identification applying this methodology in an large flexible aircraft operating in closed-loop is described in the following subsection.

3.2 Closed-loop system identification

The problem formulation consists in identify the system matrices of a discrete state-space model from input-output data. The first step to closed-loop system identification is to apply a excitation signal and to collect data, in this case using input-output data from simulation.

In the identification procedure, a maneuver using elevator as input was performed in the aircraft based on pitch-rate reference signal as shown in Fig.7. In this work, only the longitudinal dynamic is excited and is assumed whereas in straight and level cruise the longitudinal and lateral-directional dynamics are decoupled. The same flight condition presented in previous section is applied in order to obtain the closed-loop data.

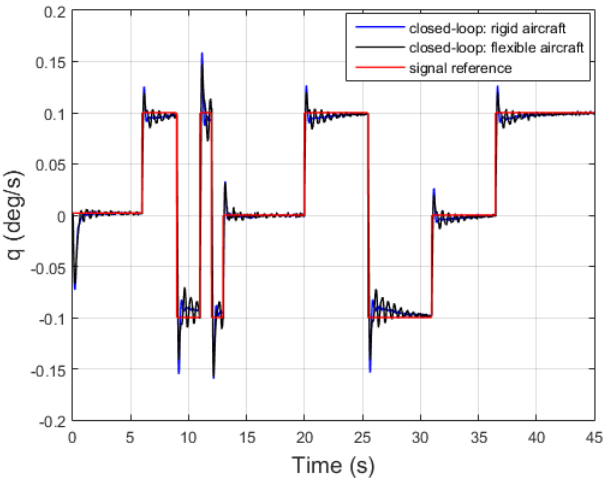

Fig. 7 Closed-loop data.

Analyzing the pitch-rate output, as shown in Fig.8, it's possible to verify the existence of an oscillation about 11.25 rad/s compared to the behavior if the aircraft is only rigid. This oscillation frequency suggests the presence of the first mode in the pitch-rate measurements.

A single control design consisting of a pitch-rate CAS [16] was implemented based on linearized matrices in order to obtain the closed-loop data. Measurements noises were added with suitable signal-to-noise ratio and the nonlinear dynamic was performed considering the five flexible modes previous described at flight condition already mentioned.

To perform the identification algorithm, a transformation of variables is necessary, such that, $d = \phi\eta$. The linear displacements d may be obtained by strain-gauges sensors located along the flexible wing and the modal shapes ϕ may be obtained from a vibration test [15]. Therefore,

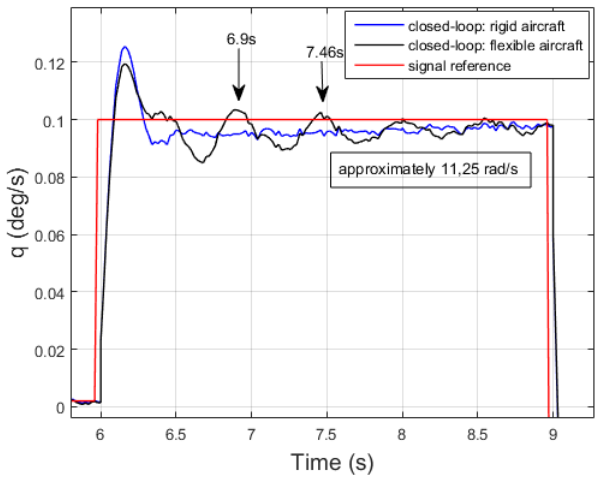

Fig. 8 Enlarged Fig.7: influence of the flexible modes.

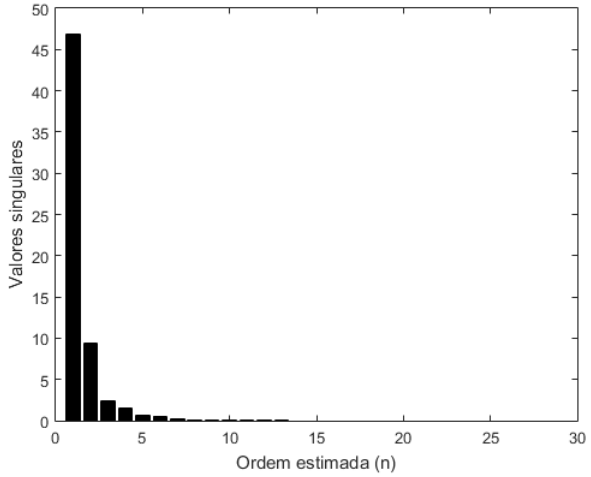

Fig. 9 Order estimation based on Singular Value Decomposition of the orthogonal projection of the future data onto the past data.

for the identification procedure is used a generalized coordinate that includes the variables η and $\dot{\eta}$.

In the system identification are used one input, four output from longitudinal dynamic and generalized displacements and velocities of the five flexible modes, in all, one input measure and fourteen output measure.

A singular value decomposition obtained with identification parameters J=30 and L=2 that corresponding at past and future horizons, respectively, is shown in Fig.9. The order n=14 was adopted to the model, based on the more representative singular values.

The model obtained from the application of SIM method can be referred as black-box model and one difficulty is to explicit the aerodynamic coefficients and the identified model have no physical meaning, but the preliminary results in this work suggest a representative model when compared with the OEM (output-error method) method well known in literature [17].

It's shown in Fig.10, Fig.12, Fig.13 and Fig.14 the Bode diagrams obtained from identified model. The results empathize that the model recovery the dynamic of aircraft along the excited frequency range without biasing.

The transfer function referred to ratio of pitch-rate to elevator deflection from identified

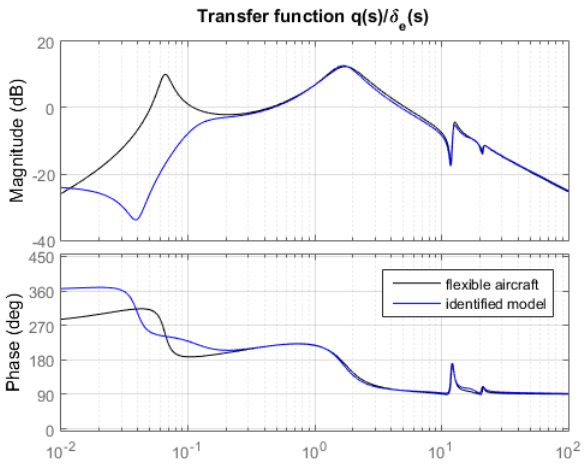

Fig. 10 Bode diagrams obtained from identified model: (a) ratio of pitch-rate to elevator deflection, $q(s)/\delta_e(s)$.

model is shown in Fig.11.

In closed-loop identification literature [8], the problems with closed-loop experiments are discussed and explained why some well known identification methods cannot be used for closed-loop identification and in closed loop generating informative data is more complicated due to the controller. Referring to the last case, the identification results of this work indicates that for low frequencies, the identified model not capture the

```
Gident1 =

  -5.6134 (s+28.13) (s+0.3858) (s+0.07844) (s^2 - 0.01153s + 0.001574) (s^2 + 13.78s + 64.61)
                              (s^2 + 0.4404s + 140.1) (s^2 + 5.705s + 311.4) (s^2 + 1.055s + 430)
  ----------------------------------------------------------------------------------------------
  (s+30.74) (s-0.08171) (s^2 + 0.1198s + 0.01343) (s^2 + 1.034s + 2.843) (s^2 + 14.13s + 68.22)
                              (s^2 + 0.9804s + 151.5) (s^2 + 5.137s + 320.6) (s^2 + 1.424s + 434.3)

Continuous-time zero/pole/gain model.
```

Fig. 11 Ratio of pitch-rate to elevator deflection, $q(s)/\delta_e(s)$, from identified model: a result by obtained via MATLAB.

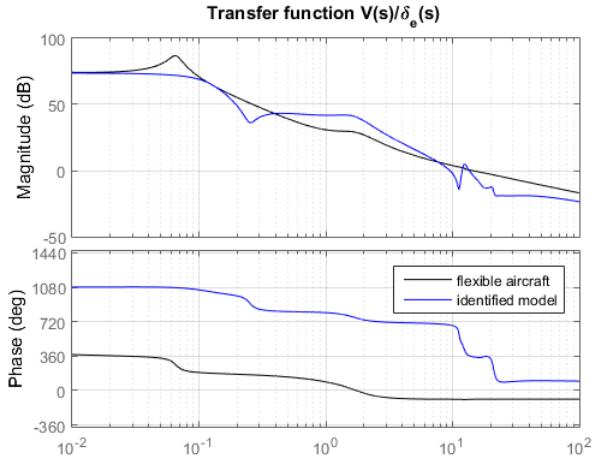

Fig. 12 Bode diagram obtained from identified model: (a) ratio of velocity to elevator deflection, $V(s)/\delta_e(s)$.

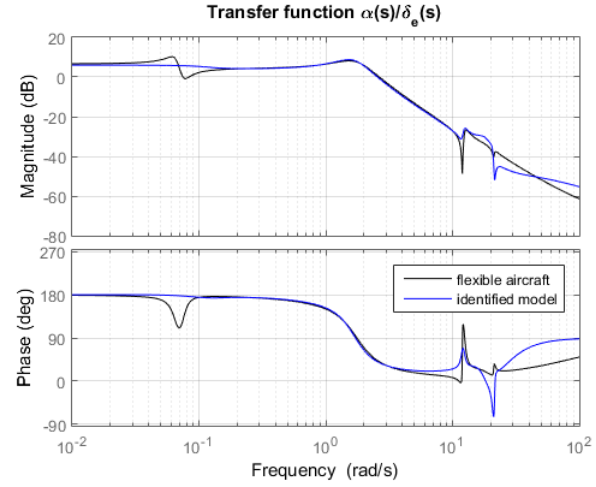

Fig. 13 Bode diagram obtained from identified model: (a) ratio of attack angle to elevator deflection, $\alpha(s)/\delta_e(s)$.

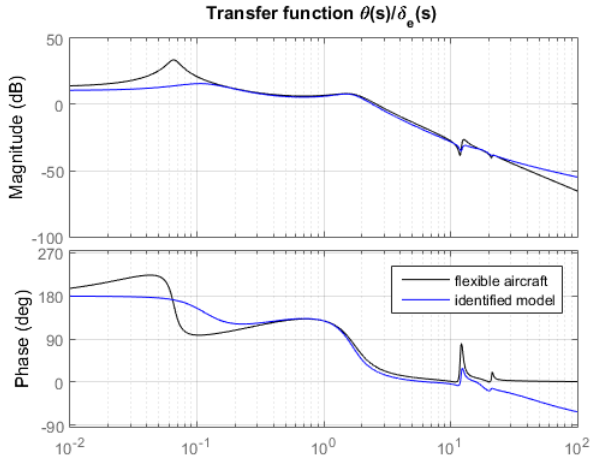

Fig. 14 Bode diagram obtained from identified model: (a) ratio of pitch angle to elevator deflection, $\theta(s)/\delta_e(s)$.

phugoidal mode and the channel between the elevator and velocity was the poorest representation suggesting a input non persistently exciting of this dynamic.

4 Conclusions

This work presents a closed-loop system identification of a large flexible aircraft well known in the literature. The goal of this work was to apply a subspace algorithm to recover the longitudinal dynamic even in presence of a feedback, that sometimes causes biasing of the estimates due to correlation between the noise and the input signal.

So, the applied algorithm avoids the biasing of estimates producing a representative discrete state-space model. The methodology presents in this work is an alternative to obtain aircraft models, using low computational efforts and not requiring an expertise in basic aerodynamics of lifting surfaces.

Another work, in progress by the authors, concerns to identify the flexible aircraft dynamics, specifically an unmanned aerial vehicle (UAV) with flexible wings, even in closed-loop operation.

Preliminary analysis obtained in this work,

show that the feedback loop produces a input non persistently exciting. So, in closed-loop systems, the identification depends of the control law and feedback variables.

Further, the future works of system identification of flexible aircrafts concerns in find a great flight test to guarantee informative data in order to recover the rigid and flexible modes.

5 Contact Author Email Address

machado@ita.br

Copyright Statement

References

[1] B.G.O. Silva and W. Mönnich, *System identification of flexible aircraft in time domain*, AIAA Atmospheric Flight Mechanics Conference (2012).

[2] B.G.O. Silva, *Data gathering and preliminary results of the system identification of a flexible aircraft model*, AIAA Atmospheric Flight Mechanics Conference (2011).

[3] T. Klimmek, P. Ohme, P.D. Ciampa and V. Handojo, *Aircraft loads - an important task from pre-design to loads flight testing*, DLR, German Aerospace Center (2016).

[4] F.A. Almeida and B.G.O. Silva. *Attenuation of aircraft flexible modes during maneuvering flight*, AIAA Guidance, Navigation and Control (2013).

[5] M. Bronz and G. Hattenberger *Aerodynamic characterization of an off-the-shelf aircraft via flight test and numerical simulation*, AIAA Flight Testing Conference (2016).

[6] G. Diana and G. Fiammenghi. *Wind tunnel tests and numerical approach for long span bridges: the Messina bridge*, The Seventh International Colloquium on Bluff Body Aerodynamics and its Applications (BBAA7) (2012)

[7] T. Katayama. *Subspace Methods for System Identification: a realization approach*, Kyoto: Springer (2005).

[8] U. Forssell. *Closed-loop identification: methods, theory, and applications*, Pd.D in Electrical Engineering, Linköping University, p. 263 (1999).

[9] M.R. Waszak and D.K. Schmidt, *Flight Dynamics of aeroelastic Vehicles*, J. Aircraft, Vol. 25, No. 6, pp. 563-571 (1988).

[10] D.K. Schmidt, *A non-linear simulink simulation of a large, flexible aircraft-FLEXSIM*, Project supported by MUSYN, Inc., Minneapolis, MN, (2013).

[11] D.K. Schmidt *Modern fligth dynamics*, New York: Mc Graw-Hill (2013).

[12] D. Di Ruscio. *A Bootstrap Subspace Identification Method: comparing methods for closed loop subspace identification by Monte Carlo simulations* Journal of Modeling, Identification and Control, v. 30, n. 4, p. 203-222 (2009).

[13] R.C. Machado, *Métodos de subespaços para identificação de sistemas em malha fechada*, Master's Thesis (2013).

[14] B. De Moor and P. V. Overschee. *Subspace identification for linear sysyems: theory, implementations, applications.*, Kluwer Academic Publichers (1996).

[15] D. J. Ewins. *Modal Testing: Theory and Practice*, Published by Research Studies Ltd (1984).

[16] B. L. Stevens and F. L . Lewis. *Aircraft Control and Simulation*, Canada: John Wiley (1992).

[17] R.V. Jategaonkar, *Flight vehicle system identification*, Published by American Institute of Aeronautics and Astronautics, Vol. 216 (2006).

[18] M.R, Waszak J.B. Davidson and D.K. Schmidt, *A simulation study of the flight dynamics of elastic aircraft, results and analysis*, Vol. 2, NASA Contractor Report 4102 (1987).